Supporting Information for

Calibration-free electrochemical biosensors supporting accurate molecular measurements directly in undiluted whole blood

Hui Li[a,b,c#], Philippe Dauphin-Ducharme[b,c#], Gabriel Ortega[b,c,d] and Kevin W. Plaxco[b,c]*

[a]*Faculty of Materials Science and Chemistry, China University of Geosciences, Wuhan 430074, China*

[b]*Department of Chemistry and Biochemistry, University of California Santa Barbara, Santa Barbara, California 93106, USA*

[c]*Center for Bioengineering, University of California Santa Barbara, Santa Barbara, California 93106, USA*

[d]*CIC bioGUNE, Bizkaia Technology Park, Building 801 A, 48170 Derio, Spain*

Materials and methods

Materials

Kanamycin was purchased from Gold Biotechnology (MO, USA), doxorubicin hydrochloride salt was purchased from LC laboratories (MA, USA), 6-Mercapto-1-hexanol, tris(2-carboethyl)-phosphine hydrochloride (TCEP), and cocaine hydrochloride from Sigma-Aldrich (MO, USA); all were used as received. Bovine serum and whole blood in heparin were purchased from Hemostat Laboratories (CA, USA) and used as received. 2 and 7/8" microcloth, 1 μm monocrystalline diamond slurry (in a petroleum distillates-based slurry), and 0.05 μm

alumina powder were obtained from Buehler (IL, USA). The relevant methylene blue and thiol-modified DNA aptamer sequences (sequences as reported in references 1 and 2) were synthesized by LGC Biosearch Technologies, purified by C18 HPLC and PAGE, confirmed by HPLC profile and mass spectrometry. These were dissolved in TE buffer (1×) (10 mM tris(hydroxymethyl)aminomethane, 1 mM EDTA, pH 8.0) to a final concentration of 100 μM, aliquoted and stored at -20°C prior to use. The sequences used in this study were:

Cocaine aptamer:

5'-HO-$(CH_2)_6$-S-S-$(CH_2)_6$-AGACAAGGAAAATCCTTCAATGAAGTGGGTCG-methylene blue (MB)-3';

Doxorubicin aptamer:

5'-HO-$(CH_2)_6$-S-S-$(CH_2)_6$-ACCATCTGTGTAAGGGGTAAGGGGTGGT-MB-3';

Kanamycin aptamer:

5'-HO-$(CH_2)_6$-S-S-$(CH_2)_6$-GGGACTTGGTTTAGGTAATGAGTCCC-MB-3'

Gold electrodes (2 mm in diameter), fritted Ag/AgCl electrodes, and platinum wires were purchased from CH Instruments, Inc. (TX, USA).

To mimic the circulatory system the whole blood was circulated using a miniature gear pump (Model: GH-07012-30, Cole-Parmer; IL, USA) through a closed loop consisting of a 30 mL sample reservoir and two 4 mm-diameter and 25 cm-long plastic tubes.[1]

Sensor fabrication

E-DNA biosensors were fabricated as previously described.[2] We first polished 2 mm diameter gold disk electrodes on a micro-cloth soaked with diamond slurry followed by sonication in ethanol for 5 min. We further polished the electrodes using a micro-cloth soaked in an aqueous suspension of 0.05 μm alumina followed by sonication in water for another 5 min. After this we cleaned the electrodes electrochemically by cycling 1000 times between -0.4 and -1.35 V (all potentials versus Ag/AgCl) at 2 V s^{-1} in aqueous 0.5 M NaOH using a three-electrode setup. The working electrodes were then rinsed thoroughly with water and transferred into 0.5 M H_2SO_4 where we applied an oxidizing potential of 2 V for 5 s followed by a reducing potential of -0.35 V for 10 s followed by cycling between -0.35 and 1.5 V for 20 cycles at 4 V s^{-1} and for 4 cycles at 0.1 V s^{-1}. Finally, we determined the electroactive area of each gold electrode by integrating the area under the curve of the gold oxide reduction peak that we observed in 0.05 M H_2SO_4 using cyclic voltammetry at 0.1 V s^{-1} between -0.35 and 1.5 V and dividing it by 422 μC cm^{-2}. Freshly cleaned electrodes typically exhibit a surface area of ~0.03 (±30%) cm^2.

Immediately prior to sensor fabrication we prepared a solution of thiol-and-methylene-blue-modified DNA in phosphate buffered saline buffer (PBS; 137 mM NaCl, 2.7 mM KCl, 10 mM Na_2HPO_4, 1.8 mM KH_2PO_4, pH 7.0) by incubating a solution of 100 μM DNA and 20 mM tris-(2-carboxyethyl) phosphine hydrochloride (1:200) for 1 hr at room temperature followed by dilution with PBS to 200 nM as confirmed by UV-Vis spectroscopy. We then immersed freshly cleaned electrodes in this solution for 1 hr at room temperature. The resulting sensors were

washed with deionized water and then incubated in 20 mM 6-mercaptohexanol solution in PBS overnight at 4°C before being rinsed with water prior to use.

Electrochemical measurements

Electrochemical measurements were performed at room temperature using a CHI660D potentiostat with a CHI684 Multiplexer (CH Instruments, Austin, TX) and a standard three-electrode cell containing a platinum counter electrode and a Ag/AgCl (3 M KCl) reference electrode. Square wave voltammetry (SWV) was performed using a potential window of -0.1 to -0.4 V, a potential step of 0.001 V and an amplitude of 0.05 V.

We interrogated the cocaine-detecting sensors using 500 Hz for the traditional calibration approach (Figure 1). To define non-responsive frequency for both cocaine- and doxorubicin-detecting sensors, we interrogated the sensors by sweeping a range of frequencies from 6 Hz to 1000 Hz (Figure S3 and Figure S9). After frequency-sweeping experiments, we identified 40 Hz and 500 Hz, as non-responsive and responsive frequency, respectively, for the calibration-free operation of cocaine and doxorubicin sensors in both serum and whole blood (Figure 3 in the main text). Kanamycin-detecting sensors were interrogated in PBS, using 750 Hz and 250 Hz as responsive and low responsive frequency, respectively (Figure S15B and Figure S16).

All whole blood experiments were conducted in a closed-loop system with a continuous flow of whole blood (1 mL/s) using a circulator pump.[1] The sensors employed for continuous target monitoring (Figure 5 in the main text) were scanned every 10 s. To regenerate the sensors in these experiments, they were washed with

fresh whole blood three times.

Global fitting to determine the relevant sensor parameters

We performed data analysis using in-house built Matlab® Scripts to simultaneously fit data from all the electrodes in a given training set to Eq. 4 or Eq. 5 in order to obtain the optimized parameters α, γ and K_D. The least square errors in the fittings were propagated by Monte-Carlo analysis (10,000 steps) in order to provide a distribution of the variability in the calculated parameters α, γ and K_D.

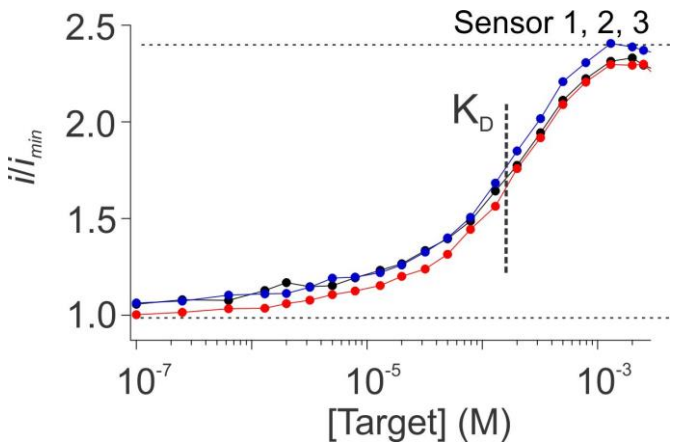

Figure S1. Calibrated electrochemical aptamer-based (E-AB) sensors. To correct for sensor-to-sensor variation in i_{min} we have historically used calibration in a target-free reference sample. We do this because, in contrast to absolute E-AB currents (Fig. 1C), the *relative* output of E-AB sensors (i/i_{min}) is, as shown here, quite reproducible.

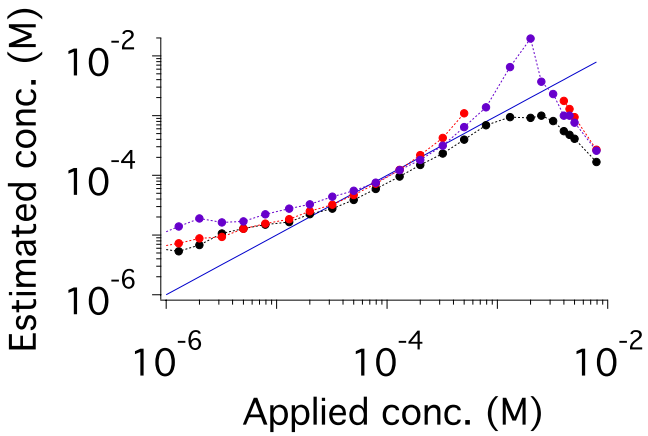

Figure S2. Accurate, precise cocaine measurements via calibration. Here we present the data for the individual sensors shown as an average in Fig. 1D. After calibration against a target-free sample these independently hand-fabricated sensors produce concentration estimates within ±10% of the actual (spiked) concentration over the range from 20 μM to 300 μM and within ±20% over the range from 10 μM to 600 μM.

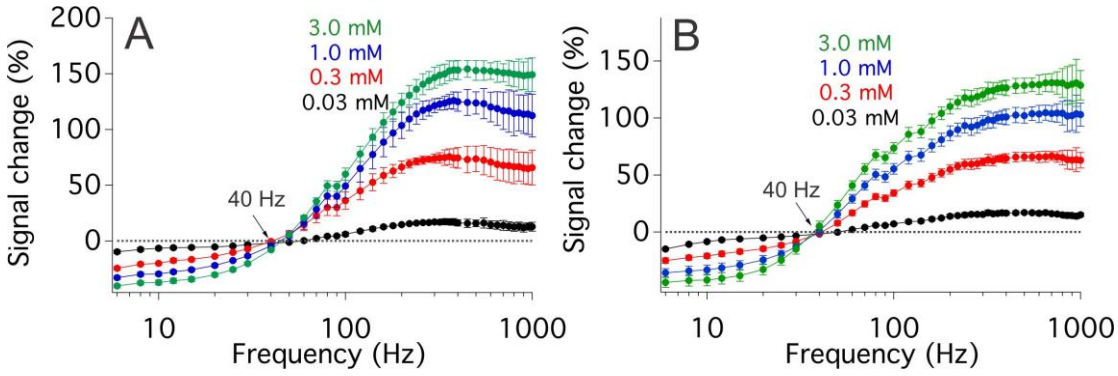

Figure S3. The non-responsive frequency of cocaine-detecting E-AB sensors. To identify f_{NR} we measured the relative output of cocaine-detecting sensors (as i/i_{min} -1) as a function of square-wave frequency when challenged in the presence of cocaine (i_{min}) and at various cocaine concentrations (i) in either (**A**) undiluted serum or (**B**) undiluted whole blood. As shown, the signal produced by this type of sensor at a

frequency of 40 Hz is independent of target concentration.

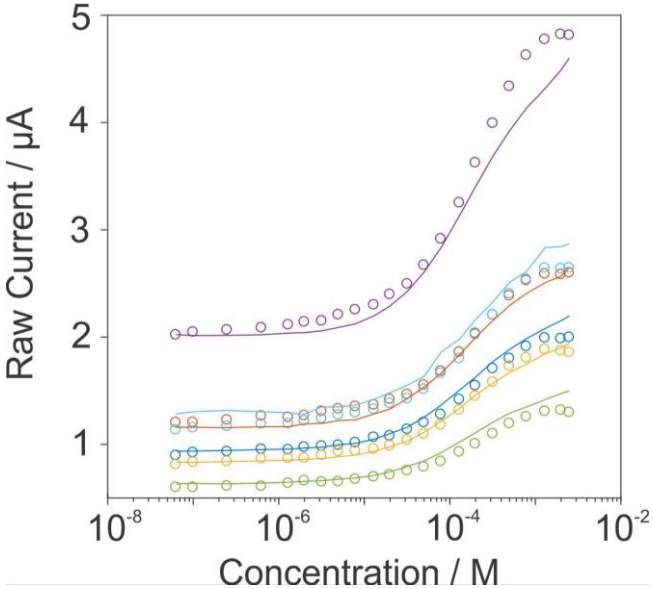

Figure S4. Global fitting of the outputs of cocaine-detecting sensors in undiluted serum. We globally fit the output of a training set of six sensors to Eq. 4 to define K_D, α, and γ for this type of sensor under these conditions. The solid lines illustrate how well the globally fit parameters describe the output of each individual sensor.

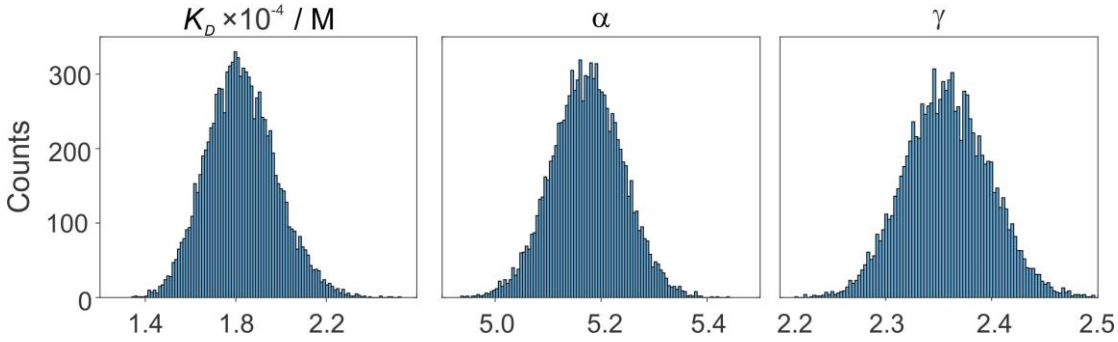

Figure S5. Optimized parameters obtained via global fitting. The squared errors in the fittings (Fig. S4) were propagated by Monte-Carlo analysis (10,000 steps) in order to provide a distribution of the variability in the calculated parameters K_D, α, and γ.

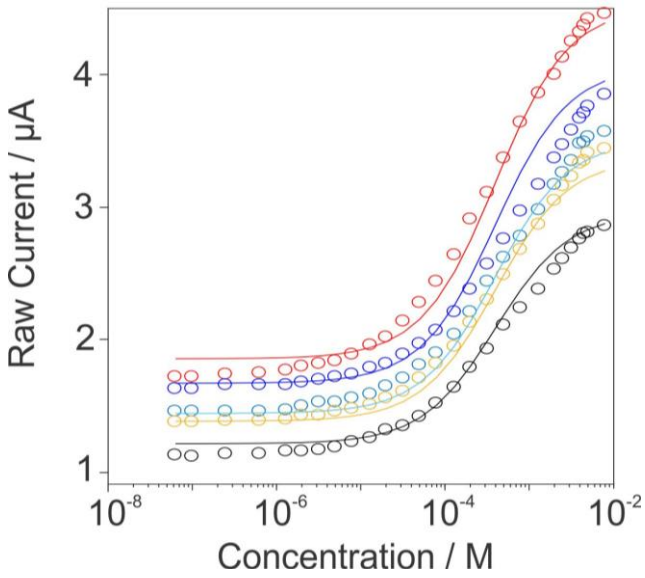

Figure S6. Global fitting of the outputs of cocaine-detecting sensors in undiluted whole blood. We globally fit the output of a training set of five sensors to Eq. 4 to define K_D, α, and γ for this type of sensor under these conditions. The solid lines illustrate how well the globally fit parameters describe the output of each individual sensor.

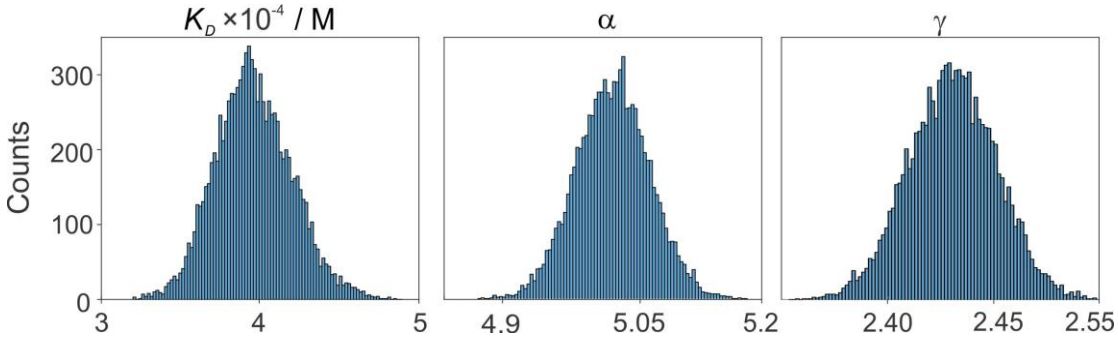

Figure S7. Optimized parameters obtained via global fitting. The squared errors in the fittings (Fig. S6) were propagated by Monte-Carlo analysis (10,000 steps) in order to provide a distribution of the variability in the calculated parameters K_D, α, and γ.

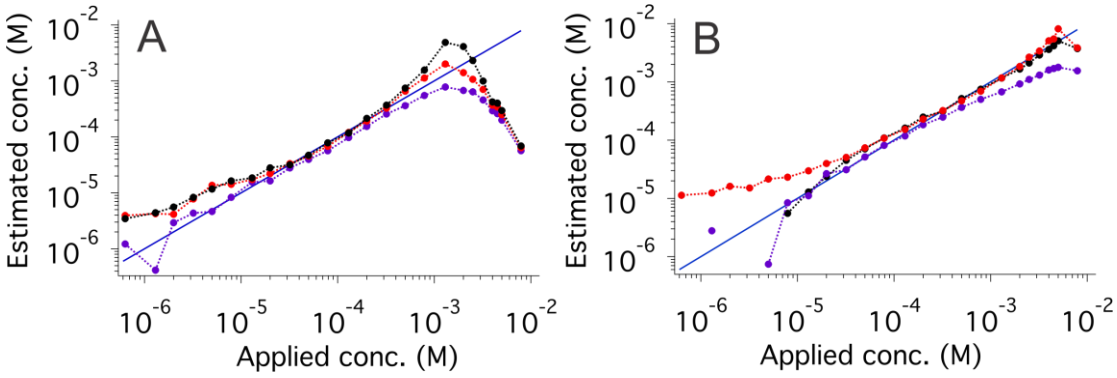

Figure S8. Accurate and precise cocaine measurements without calibration. Shown are data for the individual sensors shown as an average in Fig. 3A and B. (**A**) For example here we show three independently hand-fabricated cocaine sensors interrogated in undiluted serum, under which the estimated concentrations are accurate to within ±10% from 20 μM to 800 μM and within ±20% from 8 μM to 800 μM. (**B**) Three independently hand-fabricated sensors interrogated in whole blood are likewise accurate to within ±10% of the spiked concentrations ones over the range 60 μM to 1 mM and within ±20% over the range 20 μM to 2 mM.

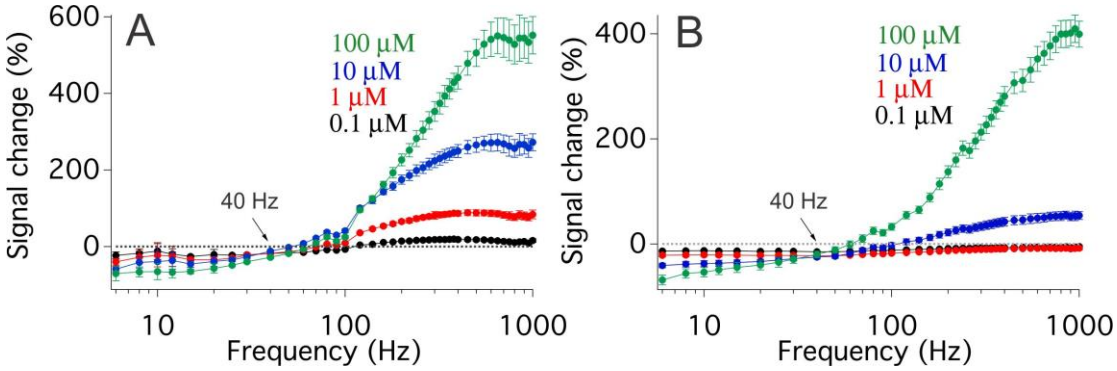

Figure S9. The non-responsive frequency of doxorubicin-detecting E-AB sensors. To identify f_{NR} we measured the relative output of doxorubicin-detecting sensors (as i/i_{min} -1) in (**A**) undiluted serum and (**B**) undiluted whole blood. As shown, the signal produced at a frequency of 40 Hz is independent of target concentration.

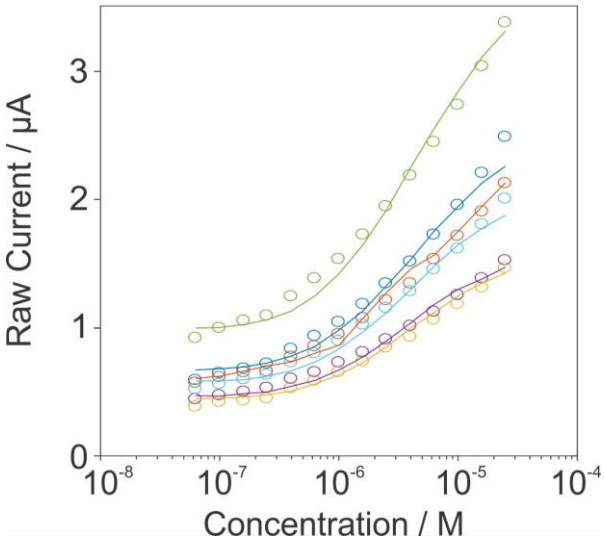

Figure S10. Global fitting of the outputs of doxorubicin-detecting sensors in undiluted serum. We globally fit the output of a training set of six sensors to Eq. 4 to define K_D, α, and γ for this type of sensor under these conditions. The solid lines illustrate how well the globally fit parameters describe the output of each individual sensor.

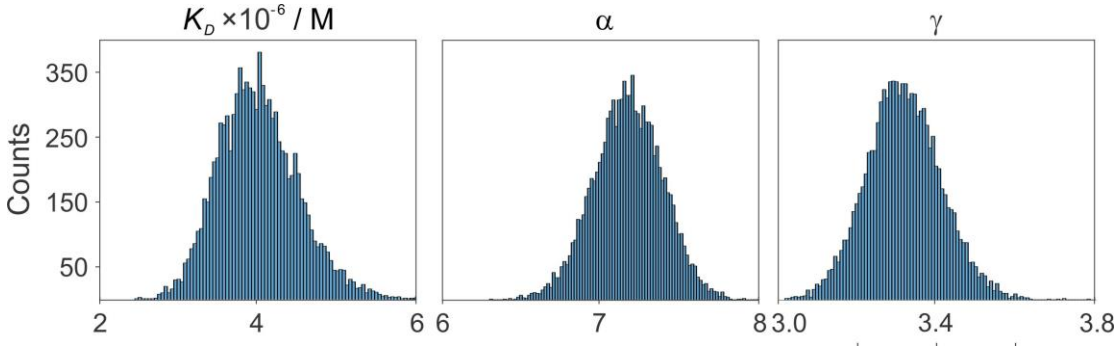

Figure S11. Optimized parameters obtained via global fitting. The squared errors in the fittings (Fig. S10) were propagated by Monte-Carlo analysis (10,000 steps) in order to provide a distribution of the variability in the calculated parameters K_D, α, and γ.

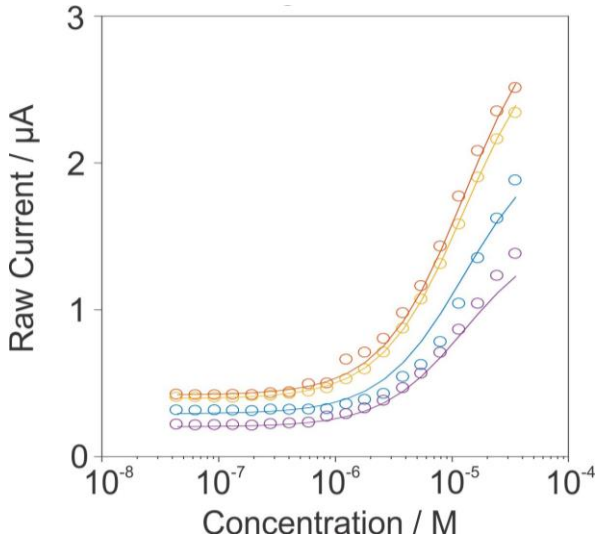

Figure S12. Global fitting of the outputs of doxorubicin-detecting sensors in undiluted whole blood. We globally fit the output of a training set of four doxorubicin-detecting sensors to Eq. 4 to define K_D, α, and γ for this type of sensor under these conditions. The solid lines illustrate how well the globally fit parameters describe the output of each individual sensor.

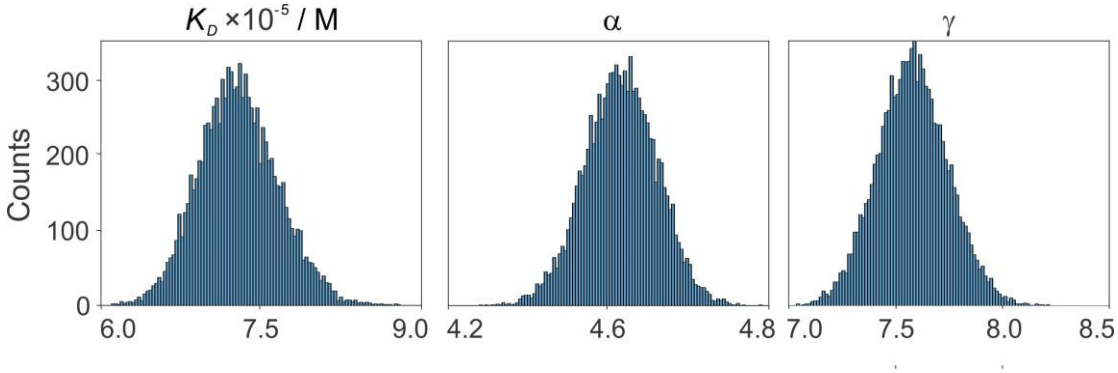

Figure S13. Optimized parameters obtained via global fitting. The squared errors in the fittings (Fig. S12) were propagated by Monte-Carlo analysis (10,000 steps) in order to provide a distribution of the variability in the calculated parameters K_D, α, and γ.

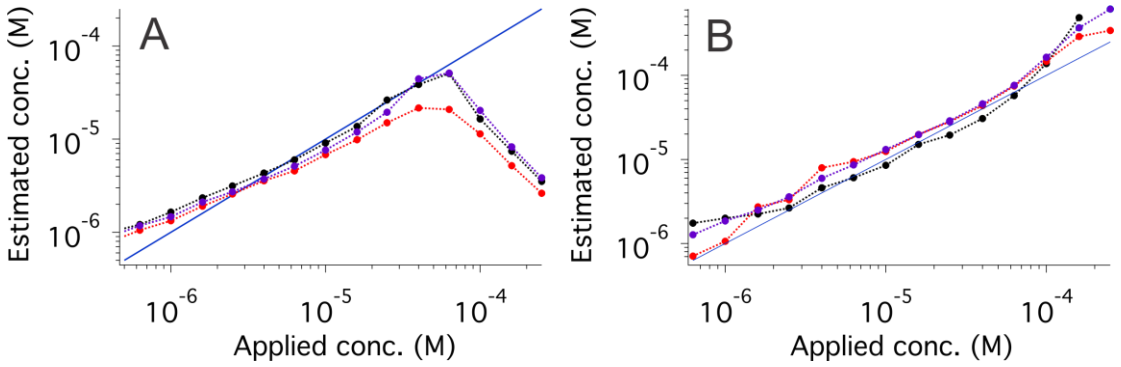

Figure S14. Accurate and precise doxorubicin measurements without calibration. Shown are data for the individual sensors shown as an average in Fig. 3C and 3D. (**A**) I.e., here we show three independently hand-fabricated sensors interrogated in undiluted serum, under which the estimated concentrations are accurate to within ±10% from 2.5 μM to 6 μM and within ±20% from 2 μM to 40 μM. (**B**) Three independently hand-fabricated sensors interrogated in whole blood are likewise accurate to within ±10% of the spiked concentrations over the range 10 μM to 60 μM and within ±20% from 4 μM to 100 μM.

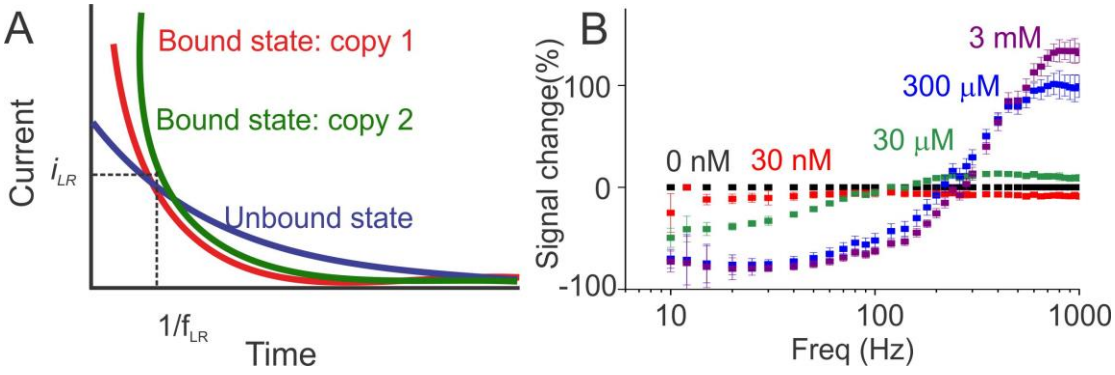

Figure S15. Multi-phase binding reduces the likelihood of there being a non-responsive frequency. (A) If some third binding phase were significantly populated it would produce a third decay curve when the sensor was interrogated with a square-wave potential pulse. Because it is unlikely that all three current decays would cross at a single point, it is unlikely that there will be a non-responsive frequency at which the sensor output is independent of target concentration. **(B)** For example, the kanamycin aptamer exhibits a second binding event at high target concentrations (Fig. 4 and Fig. S16), rendering the sensor output dependent on target concentration at all square-wave frequencies. At 250 Hz, however, the output is only minimally responsive to the target (Fig. 4).

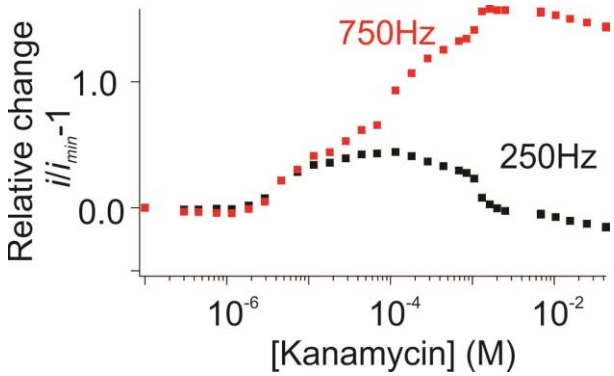

Figure S16. Relative signal outputs for a kanamycin-detecting sensor. The downturn in sensor output at high target concentrations presumably reflects an additional binding event that further alters the aptamer's conformation.

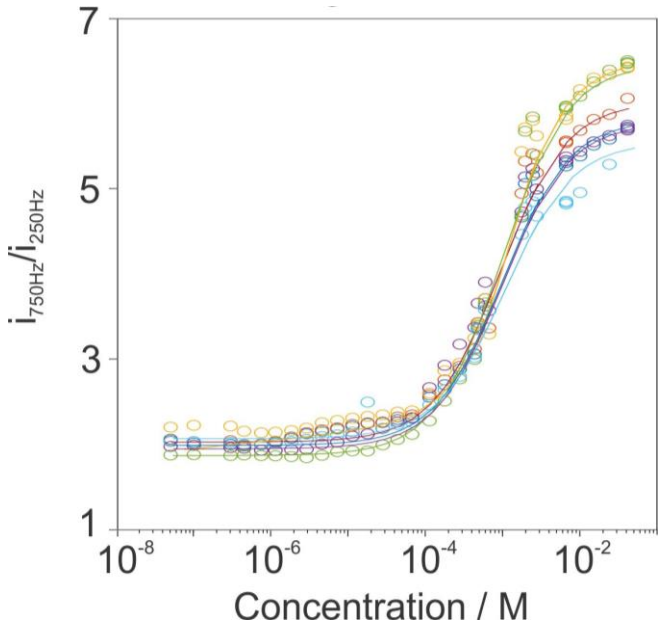

Figure S17. Global fitting of the output of kanamycin-detecting sensors in PBS. We globally fit the output ratio $i_{750\,\mathrm{Hz}}/i_{250\,\mathrm{Hz}}$ of a training set of six sensors to Eq. 4 to define K_D, α, and γ for this type of sensor under these conditions. The solid lines illustrate how well the globally fit parameters describe the output of each individual sensor (Fig. 4B).

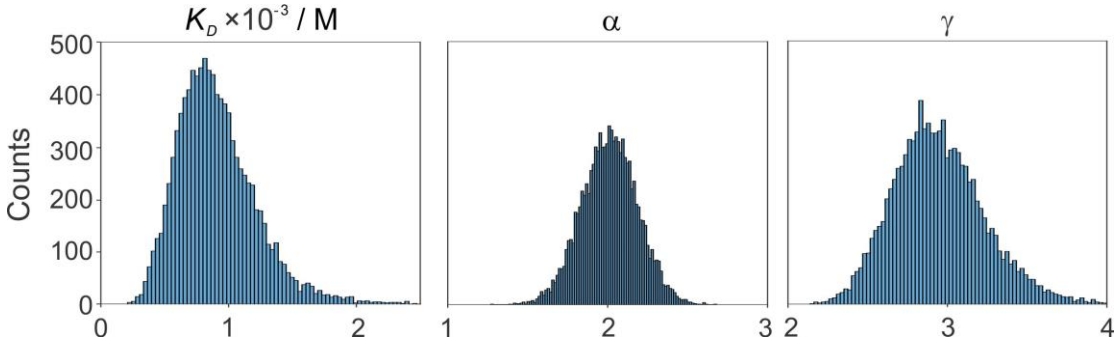

Figure S18. Optimized parameters obtained via global fitting. The squared errors in the fittings (Fig. S17**)** were propagated by Monte-Carlo analysis (10,000 steps) in order to provide a distribution of the variability in the calculated parameters K_D, α, and γ

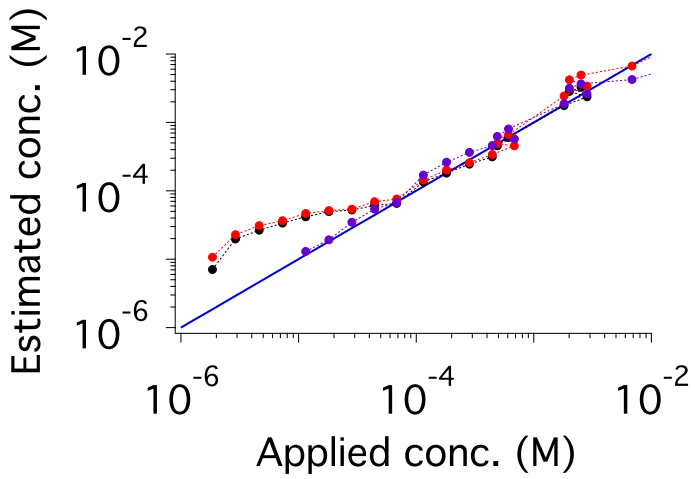

Figure S19. Accurate and precise kanamycin measurements without calibration. Presented here are data for the individual sensors shown as an average in Fig. 4C. We obtain calibration-free estimates of kanamycin concentration in buffer that are accurate to within ±10% over the range 40 μM to 1 mM and within ±20% over the range 30 μM to 3 mM.

Table S1. The parameters α, γ and K_D for the E-AB sensors

Aptamer / Parameters	Cocaine		Doxorubicin		Kanamycin
	Serum	Blood	Serum	Blood	PBS
α	5.17	5.04	7.16	4.70	2.03
γ	2.34	2.43	3.31	7.46	2.97
K_D	182 μM	395 μM	3.98 μM	69.2 μM	920 μM

References

1. Li, H., Arroyo-Currás, N., Kang, D., Ricci, F. & Plaxco, K.W. *J. Am. Chem. Soc.* **2016,** *138*, 15809-15812.
2. Xiao, Y., Lai, R. Y. & Plaxco, K. W. *Nat. Protoc.* **2007,** *2,* 2875-2880.